Jour. Geol. Soc. India (2022) 98:815-821
https://doi.org/10.1007/s12594-022-2072-4

ORIGINAL ARTICLE

Magma Mixing and Mingling during Pluton Formation: A Case Study through Field, Petrography and Crystal Size Distribution (CSD) Studies on Sirsilla Granite Pluton, India

Ch. Ashok[a,*], G.H.N.V. Santhosh[a], Sarbajit Dash[a,b] and J. Ratnakar[c]

[a]CSIR-National Geophysical Research Institute, Uppal Road, Hyderabad - 500 007, India
[b]Academy of Scientific and Innovative Research (AcSIR), Ghaziabad - 201 002, India
[c]Deportment of Geology, Osmania University, Hyderabad - 500 007, India
***E-mail:** ashokchadp@gmail.com*

Received: 7 April 2021 / Revised form Accepted: 17 January 2022

ABSTRACT

Field, petrography, and crystal size distributions (CSD) of different lithological variants from Sirsilla granitic pluton (SGP), southern India, is described here to understand operative magmatic processes. The SGP contains many mafic microgranular enclaves (MMEs) and syn-plutonic dykes. The contact relationship between MMEs and the host granite is often diffusive or gradational and rarely sharp, implying disaggregation and under-cooling of MMEs. Petrographic features like resorption textures, quartz ocelli, and the poikilitic nature of the large K-feldspar grains enclosed within plagioclase indicate interaction and magma mixing/mingling processes in an open magma chamber. Bladed biotite and acicular apatite grains in MMEs are due to rapid crystallization during the magma mingling process. The CSD curves generated for plagioclase provide an inverse relationship between population density and crystal size. Multiple crystal populations, i.e., a gently sloping line for the core samples and a steeply sloping line for margin samples, are interpreted to be caused by the mafic - felsic magma mixing and mingling processes.

INTRODUCTION

Mafic microgranular enclaves (MMEs) are important rock associations in many granitic plutons, which are of help to understand the magmatic processes in crustal-level magma chambers. Therefore, the field, petrography, geochemistry, and mineralogical characteristics of MMEs and their host rocks are crucial for examining the origin and evolution of granitoids (Barbarin and Didier 1992; Barbarin 2005; Wiebe and Hawkins 2015). Similar studies are also available in the Indian context (Jayananda et al. 2014; Elangovan et al. 2017; Kumar et al. 2017; Shukla and Mohan 2019; Kumar 2020). Despite such studies, the genesis of MMEs is still debatable. Magmas parental to mafic microgranular enclaves (MMEs) are considered to be essentially derived from a mantle source. This component seems to have interacted with granitic melts from the crust to develop hybrid calc-alkaline rocks while generating a large granite body (Castro et al. 1990). Most of the researchers conclude that MMEs are produced by magma mixing and mingling process based on field, petrographic and geochemical studies, which are confined to calc-alkaline felsic intrusions (Frost and Mahood 1987; Barbarin and Didier 1992; Arvin et al. 2004; Barbarin 2005; Kumar, 2010, 2020; Perugini and Poli 2012; Jayananda et al. 2014).

Such mixing of magmatic components in different proportions plays a significant role in the compositional diversity of the granitoid plutons (Wiebe and Hawkins 2015) and is controlled by factors like rheology, crystallinity, temperature, and composition (Barbarin 1990, 2005; Perugini et al. 2003) of the interacting magmas. The magma mixing/mingling also contributes to the disequilibrium conditions, which impact the nucleation and growth rates of the crystals (Slaby, 2004). Crystal size distribution (CSD) in felsic magmas is considered significant for inferring the paragenesis of different mineral species as the magma evolves during dynamic magma chamber processes (Cashman and Marsh 1988; Marsh 1998; Deb and Bhattacharyya 2018). As part of the current study, to understand the chamber processes that operated during the pluton evolution. Here, field, petrographic, and CSD analyses was carried out from the Sirsilla granitic pluton in the north-western part of the eastern Dharwar craton (EDC), India.

GEOLOGICAL SETTING

The Dharwar craton of southern India contains a considerable volume of granitic rocks. The western and eastern segments of the Dharwar craton display distinctly different phases of granite emplacement. The 3.35-3.3 Ga poly-phase tonalite-trondhjemite granodiorite (TTG) suites dominate the western Dharwar vraton (WDC) compared to the 2.7-2.5 Ga calc-alkaline granitic rocks of the eastern Dharwar craton (EDC) where some older remnant granites preserved (3.3–3.0 Ga) (Meen et al. 1992; Jayananda et al. 2020). Two major episodic events in the EDC include large volcanic-dominated greenstone belts at 2.7 – 2.54 Ga (Manikyamba et al. 2009; Manikyamba and Kerrich, 2012) and extensive North-South trending calc-alkaline plutonic bodies at 2.57-2.52 Ga (Dey 2013; Jayananda et al. 2013). The Karimnagar granulite belt (KGB) from EDC accommodates several smaller granitic plutons that run along the NW- SE trending Pranahita-Godavari rift basin (Fig. 1b). The KGB usually consists of granite gneisses associated with charnockite, enderbite, banded magnetite quartzite (BMQ), and dolerite dykes (Rajesham et al. 1993; Meshram et al. 2021). The Sirsilla granitic pluton (Fig. 2) is emplaced into the KGB. The distorted mushroom-shaped intrusion cross-cuts the regional NNE-SSW trend suggesting that it is a younger intrusion. The KGB in the region consists of the tonalite-trondhjemite granodiorite (TTG) suite of the peninsular

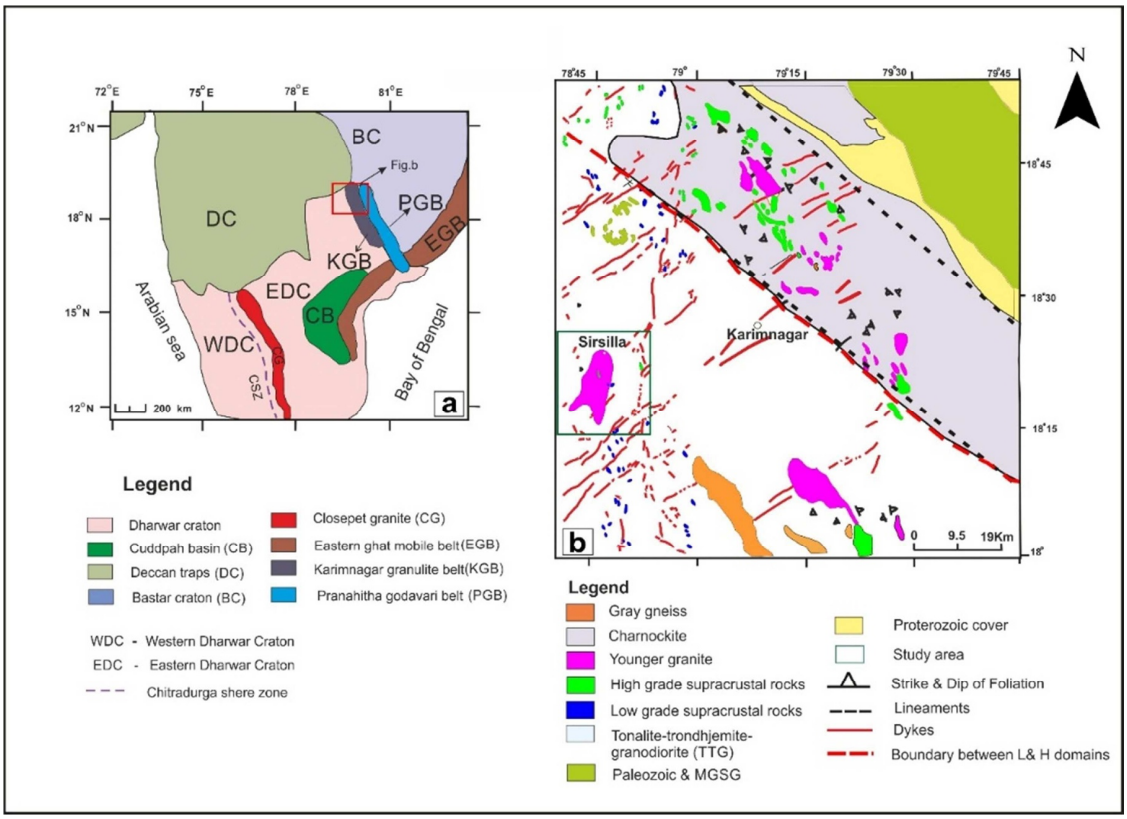

Fig.1. (a) Generalized geological map of Dharwar Craton, southern India. **(b)** Detailed geological map of Karimnagar granulite belt (KGB).

gneissic complex of the EDC. Regionally, the study area is also intruded by numerous basic dykes that do not extend into the SGP, suggesting that the intrusion of SGP postdates dyke activity in the Sirsilla area.

FIELD RELATIONS

Granite

The granitic rocks of the SGP are largely pinkish and grey colour. The pink granite is coarse- to medium-grained equigranular biotite-bearing monzogranite to syeno-granite. The grey granite is coarse- to medium-grained with equigranular to in equigranular textures and compositionally biotite-bearing granodiorite. The K-feldspar crystals (Fig. 3d) are 2-5 cm in dimension; epidote veins intrude into the interior of the granite and mafic microgranular enclaves (MMEs).

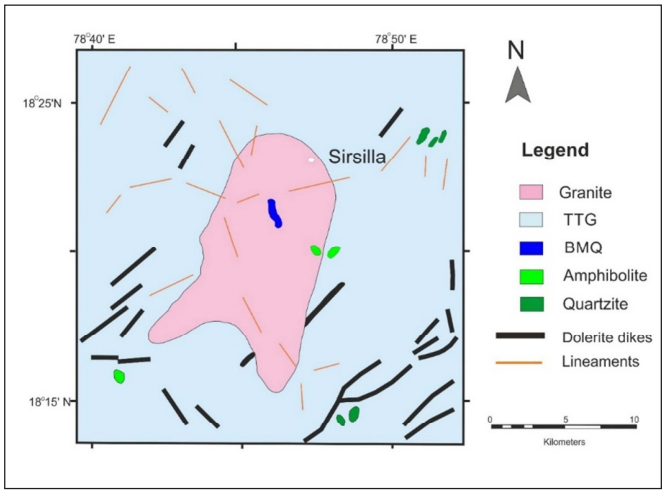

Fig.2. The sketch geological map of Sirsilla granite pluton (SGP) (modified after GSI 1996). TTG: Tonalite-trondhjemite-granodiorite; BMQ: Banded-magnetite-quartzite.

Mafic Microgranular Enclave (MME)

In the SGP, MMEs are found to be abundant along the periphery of the pluton. However, very few are present in the core of the pluton, which is possibly connected to vigorous convection in the magma chamber. The MMEs are rounded to stretched or pillowed-shaped bodies with clear magmatic features (Fig.3 a, b, c, and d). They are usually darker and fine-grained in contrast to their host granites. They range from 5 to 20 cm in diameter but are occasionally noticed between 20 and 50 cm in diameter ones. Different stages of the hybridization processes with increasing degree of magma mixing, as seen in the field, are shown in (Fig.3a to d). The MMEs are oval to sub-rounded, sharing sharp contacts with the host granite (Fig. 3a and b), signifying quenched mafic blobs in crystallizing felsic hosts. Whereas some of the MMEs are medium-grained and rounded to oval-shaped (Fig. 3c and d), having diffusive contact with the host rock. The early formed K-feldspar crystals intruding into the MME from the crystallized host granite (Fig. 3d). This suggests that the host granite was solidified at the time of mafic magma injection. Hybridization of felsic and mafic units was also observed (Fig. 3e and Fig. 3f). Such features are largely observed along the periphery of the pluton. Schlieren of mafic and felsic facies impart layering-like features in such horizons in the outcrops (Fig. 3e. and Fig. 3f).

Syn-plutonic Dykes

Syn-plutonic dykes injected into crystallizing felsic magma chambers were reported earlier from the Phanerozoic calc-alkaline plutons in arc environments (see Barbarin, 2005; Jayananda et al., 2009; Prabhakar et al., 2009). They exhibit magmatic foliation parallel to the host granite. Here, similar occurrences are found from SGP. These dykes display sharp (Fig. 4a), cuspate, and lobate (Fig. 4b and

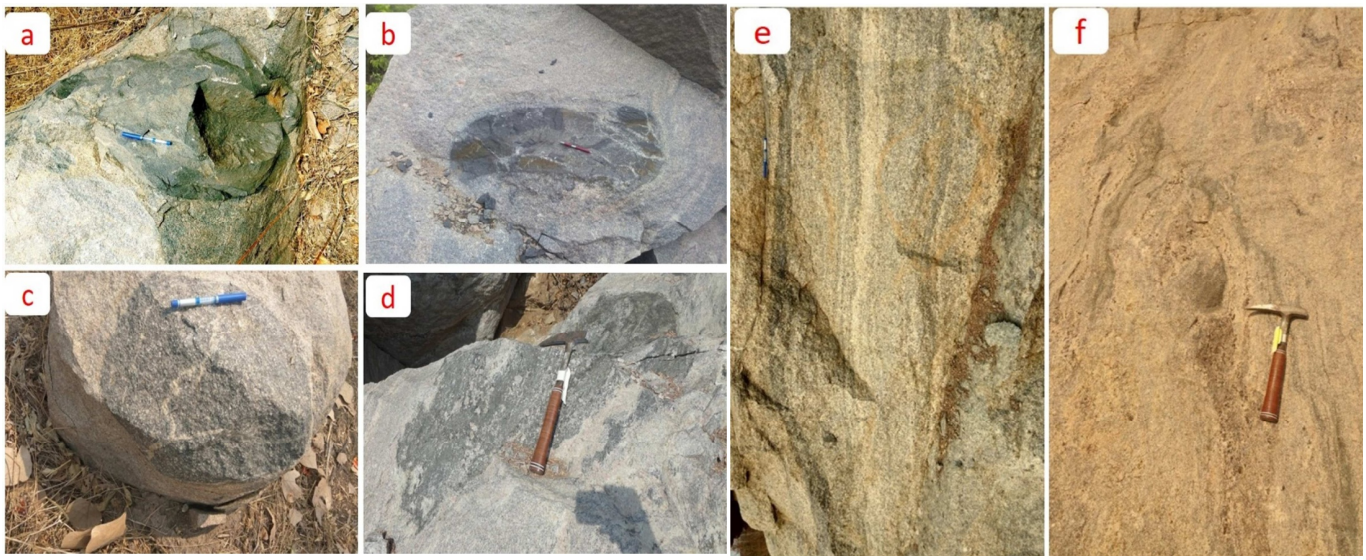

Fig. 3. (a) Ellipsoidal or sub-rounded MMEs were enclosed within the host granite. **(b)** Sub-rounded or oval-shaped MME associated with chilled margin surrounded host granite. **(c)** Rounded MME consisting of small felsic clots and felsic vein. **(d)** The presence of early formed K-feldspars injected into the MME from the crystallized host granite. **(e)** Mafic layers and host granite define magmatic flow about 10 km east of Sirsilla town at Venkatapuram village. **(f)** Schlieren structures are developed along the margins of the pluton.

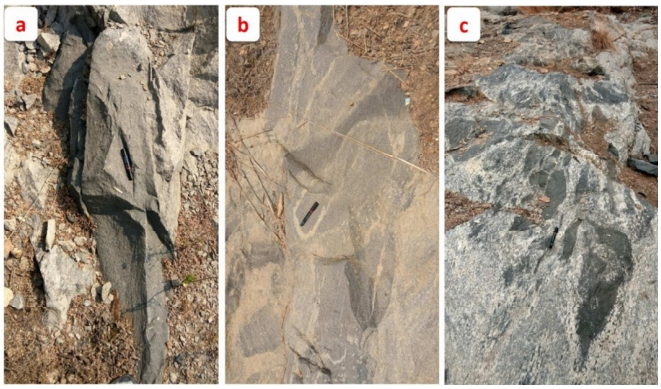

Fig. 4. (a) The continuous syn-plutonic dyke shows sharp contact with host granite. **(b)** Syn-plutonic dyke possesses alkali feldspar crystals and is back veined with host granite towards the margin of the pluton. **(c)** Mafic clots and disrupted syn-plutonic dike display diffusive contact with host granite near Jillela village.

c) contacts with host granite characterized by necking and also back veining (Fig. 4b). These dykes commonly exhibit fine- to medium-grained, equigranular to porphyritic textures, and their thickness ranges from 5 to 25 meters.

PETROGRAPHY

The host Sirsilla granitic rocks are coarse- to medium-grained and show equigranular, hypidiomorphic, and porphyritic textures. Quartz, K-feldspar, plagioclase feldspar, and biotite are the dominant minerals, with apatite, titanite, and zircon as accessory minerals. Intergrowth textures such as perthite, poikilitic, and myrmekitic were also observed in host granite. Microcline shows crosshatched twinning with inclusions of quartz (Fig. 5a and b). Plagioclase grains within the granite also enclose quartz grains (Fig. 5b). Textural features of syn-plutonic dyke and MMEs suggest the coeval nature of felsic and mafic magmas. Major minerals of syn-plutonic dyke and MMEs include biotite, hornblende, plagioclase, and K- feldspar. Accessory minerals include epidote, apatite, titanite, and opaques. Plagioclase in MME displays moderately developed twinning with sericitization (Fig. 5c). Epidote is an alteration product of plagioclase in the syn-plutonic dykes (Fig.5d), especially in peripheral samples. Biotite, amphibole, and feldspar exhibit preferred orientation in MMEs (Fig. 5e). Plagioclase exhibits resorbed surface in MMEs (Fig. 5f).

Poikilitically enclosed alkali feldspar and quartz are observed in hornblende, biotite, plagioclase within MMEs, and syn-plutonic

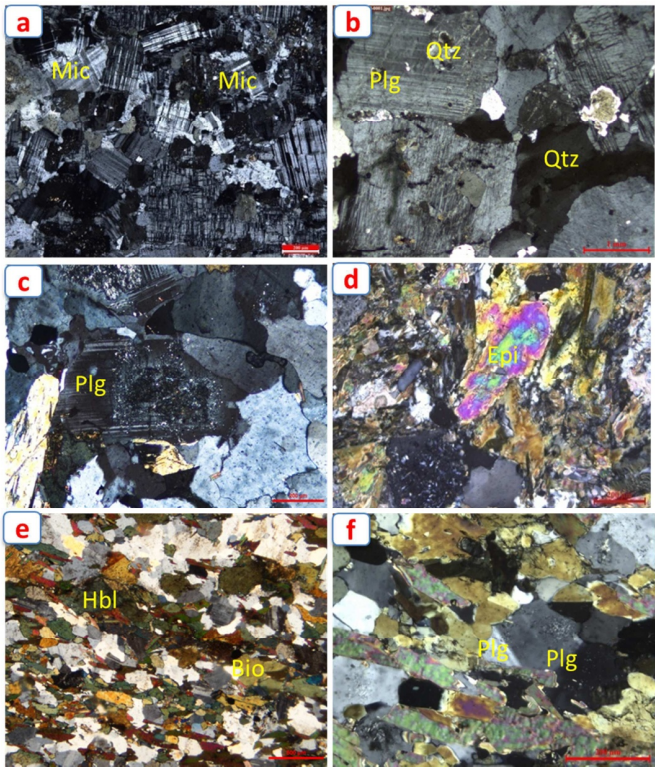

Fig. 5. Petrographic features of the SGP. **(a)** Microcline showing cross-hatched twinning in the host granite. **(b)** The Poikilitically enclosed quartz is observed in plagioclase feldspars, and also quartz grain exhibits undulose extinction in the host granite. **(c)** Plagioclase feldspars display moderate twining and initial stage of sericitization in the MME. **(d)** Epidote is an alteration product of plagioclase with tiny zircons in the syn-plutonic dike. **(e)** The preferred orientation of mafic minerals such as biotite and amphibole with feldspar in MME. **(f)** Plagioclase exhibits resorbed surfaces in the mafic magmatic enclave.

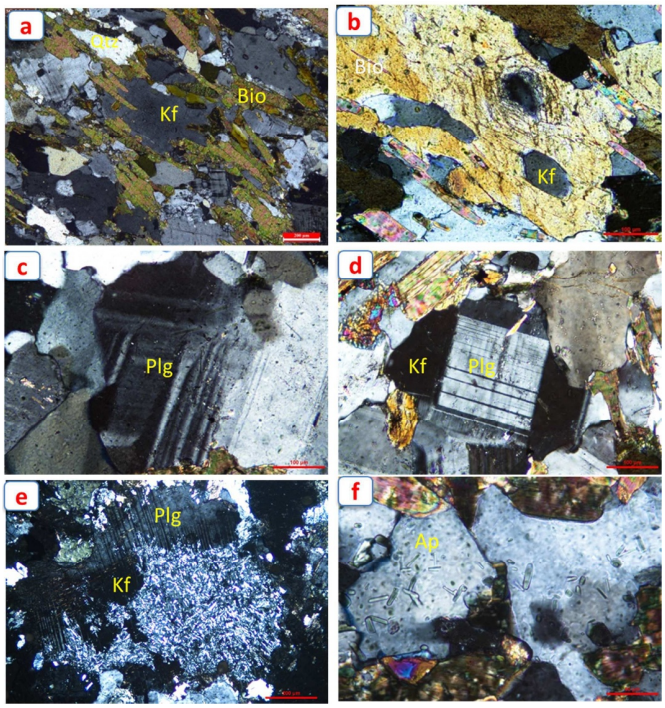

Fig. 6. **(a)** Alkali feldspar grains poikilitically enclosed on biotite in the mafic magmatic enclave. **(b)** Quartz ocelli and alkali feldspar ocelli are encompassed by bladed biotite in the syn-plutonic dike. **(c)** Plagioclase showing oscillatory zoning in MME. **(d)** The alkali feldspar is mantled by early formed plagioclase in the MME. **(e)** Mantling of alkali feldspar on plagioclase feldspar grain in MME. **(f)** Random oriented acicular apatite inclusions in alkali feldspar in MME.

dykes (Fig. 6a). Ocellar texture (Fig. 6b) is exhibited by quartz and alkali feldspar crystals, encompassing bladed biotite and hornblende in MMEs and syn-plutonic dyke. Frequently, plagioclase crystals show oscillatory zoning in the MMEs and syn-plutonic dyke (Fig. 6c). Alkali feldspar is mantled by early formed plagioclase feldspar (Fig. 6d). Alkali feldspar encompassed by dendritic plagioclase suggests that high-temperature plagioclase develops around the alkali feldspar, giving rise to rapakivi texture (Fig.6e). Acicular prismatic apatite crystals were also observed in the alkali feldspar and quartz within the MMEs and syn-plutonic dike (Fig.6f).

CRYSTAL SIZE DISTRIBUTION STUDY

The concept of crystal size distribution was first introduced (Cashman and Marsh 1988; Marsh 1998) to understand the magma dynamics in terms of plagioclase crystallization and growth rate during magmatic evolution. The variation of the natural logarithm of the crystal population density (i.e., the number of crystals per unit volume) with the crystal size (L) provides a linear pattern under a consistent state of the open system. The slope of the CSD curve (Tr) provides the average growth rate of the crystal (G)×residence time (ô) with the equation Tr =1/Gô, where intercept value and crystal length provide nucleation density (Marsh 1998; Higgins and Roberge 2007). CSD diagram displays straight lines that suggest their consistent conditions of magma (Higgins 2002). It is suggested that a set of straight lines along the same slope yet varies in intercepts generated by reducing temperature. Also, a longer residence time modifies the CSD slope but inhibits the same intercept value. The steeper slope shows evidence of crystal fractionation. According to Higgins (1996), the curved concave up CSD strongly suggest the magma mixing process. Besides, curved CSD is generated as a result of the progressive period of cooling through the ascent and the emplacement of magma (Armienti et al. 1994).

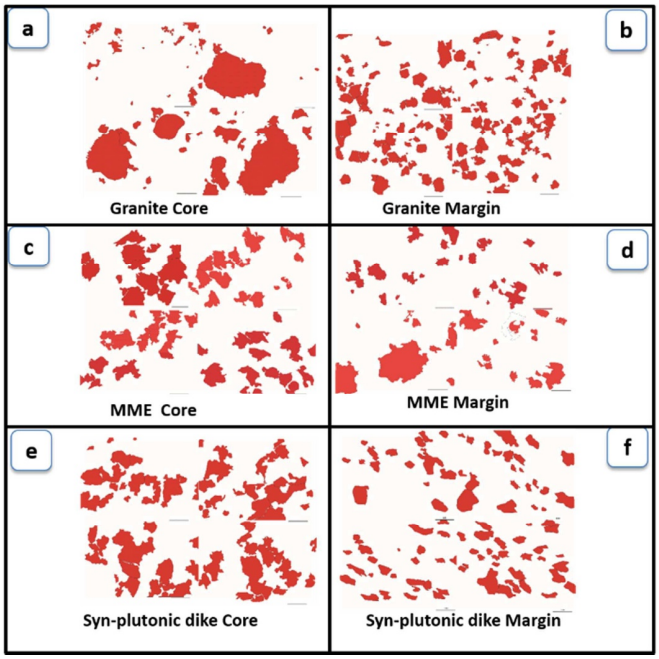

Fig. 7. Digitized outlines of **(a–b)** red-colored haphazardly oriented plagioclase grains present in host granite; **(c-d)** MME; **(e-f)** syn-plutonic dike.

In studying CSD parameters concerning the magma dynamics, thin sections of selected litho-samples were observed under a petrological microscope for textural variations. Polarized light images were obtained using a petrological microscope, especially for plagioclase grains (Fig.7). The measurements of the long axis of individual plagioclase feldspar crystals gave consistent curves for the litho units of the SGP. The natural logarithm of crystal population density versus crystal length was plotted for the plagioclase grains from the SGP (Fig. 8). The crystal population density of granites, MMEs, and Syn-plutonic dyke range from 3 to -5.52, 0.4 to -4, and 0.4 to 3.2, respectively. The CSD curves of SGP samples exhibit straight to curved patterns. Table 1 incorporates values for the slope and intercept values of different plagioclase populations calculated from CSDs of SGP. According to (Garrido et al. 2001), the development of the plagioclase crystal population is 10^{-10} mm s^{-1} for shallow depth level igneous intrusions. Additionally, residence time can be calculated

Table 1. Crystal size distribution (CSD) parameters of plagioclase for host granite, MME, and syn-plutonic dike.

Sl. No.	Plagioclase in rock types	Goodness of fit (Q)	Intercept (proportional to nucleation density	Slope	Characteristic length in mm	Residence time (year)
1	Granite core (MU-15)	0.75	0.063	-1.487	0.672495	213.4905
2	Granite margin (J-19)	0.70	2.665	-1.483	0.594177	188.6276
3	MME Core (MU-25)	0.81	0.697	-1.595	6.626959	199.0347
4	MME margin (AMP-1)	0.78	0.092	-1.848	0.541126	171.7859
5	Syn-plutonic dike core (J-11)	0.51	2.355	-1654	0.604595	191.9349
6	Syn-plutonic dike margin (SG-13)	0.68	3.357	-1.866	0.535906	170.1288

from the growth rate, assuming that the growth rate of plagioclase is 10^{-10} mm s^{-1} (Cashman 1993).

DISCUSSION

Interaction of Coeval Ffelsic-mafic Magmas

The interaction between coeval felsic and mafic magmas is strongly depended on their initial temperatures, relative volumes, and degree of crystallinity, water contents, and viscosities (Wyllie 1977; Frost and Mahood 1987; Barbarin 2005). During the initial stages of mafic magma injection into the crystallizing felsic host, a strong rheological difference may occur between felsic and mafic magmas, which restricts large-scale interactions. In this physical interaction process, there is a minimal decrease in the thermal and rheological divergence of both magmas, leading to the injection of crystals from felsic host magma into mafic magma and distributions of mafic magma into the felsic host as enclaves (Sparks and Marshall 1986; Poli et al. 1996). The MMEs, circular to ellipsoidal shape blobs, with sharp contacts and chilled margins, are formed due to viscosity contrast between the felsic and mafic magmas during the injection of mafic component into the felsic host (Barbarin and Didier, 1992; Perugini et al., 2004). The viscosity contrast was developed due to the mixing of a high viscous partially crystallized granitic pluton with a high temperature, low viscous mafic melt. The very initial stage was characterized by disequilibrium mixing of the two magma components, gradually leading to a viscosity normalization and equilibrium reaction at a later stage. The rounded and elongated shape of the MMEs in the host granite suggests the viscosity contrast between the mafic and felsic components during the magma mixing and mingling process (Fig. 3a, c). The K-feldspar crystals associated with MMEs (Fig. 3d) and syn-plutonic dykes (Fig. 4b) suggest that the already developed crystals were incorporated from solidifying felsic host (Barbarin and Didier, 1992; Kumar et al., 2004). The felsic crystals of different volume proportions and shapes are evident due to their partial dissolution and overgrowth. Fine-grained chilled margins associated with MMEs (Fig. 3b) demonstrate that the high-temperature mafic magma was undercooled, while getting injected into the moderately cooled solidifying felsic host (Kumar 2010). Flow structures appear due to magmatic flow amid magma solidification, typically attributed to schlieren structures (Barbarin and Didier, 1992; Elangovan et al., 2017). The presence of MMEs largely confined to the periphery of the granitic with diffused contacts further corroborates the mixing and mingling of the different magma variants (Fig. 3e and f). The syn-plutonic dyke emplacement also appears to have been controlled largely by the magma flow in the magma chamber. The syn-plutonic dykes, along with mafic clots (Fig.4c), display a cuspate contact (Fig. 4b and c) with the host granite, which gives strong evidence for coeval nature and magma mingling (Barbarin bernard and Didier 1992; Jayananda et al. 2009; Prabhakar et al. 2009).

Petrographic features of SGP, include ocellar quartz, alkali feldspar, poikilitic K-feldspar, oscillatory zoning, resorbed surfaces, and cellular zoning in MMEs syn-plutonic dykes support magma mixing and mingling processes. Alkali-feldspar mantled by plagioclase crystal in MMEs clearly indicates the cellular zoning (Fig. 6d). The growth of cellular plagioclase crystals in MMEs is a significant indicator of thermal quenching, formed amid the mixing process (Hibbard 1981, 1991; Barbarin 1990; Jeen et al. 2002; Jayananda et al. 2014; Vernon 2016). The K-feldspar mantled by plagioclase crystal representing rapakivi texture (Fig. 6e) is a significant sign of rapid cooling amid magma mixing conditions (Jeen et al. 2002; Vernon 2016). Resorbed surfaces in plagioclase (Fig. 5f) suggest their stability is affected due to the rapid undercooling and magma mixing process (Hibbard 1981). The ocelli textures of alkali feldspar and quartz were noticed in marginal MMEs (Fig. 6a) and syn-plutonic dyke of SGP. Rapid crystallization of hornblende and biotite mantled by dissolved quartz and alkali feldspar represents ocelli textures that developed due to the interaction of introducing mafic magma with the felsic host (Hibbard 1991; Vernon 1991; Baxter 2002). Occasionally, poikilitic quartz and alkali feldspar were noticed in biotite (Fig.6b), which occur due to the incorporation of early-formed alkali feldspar and quartz of solidifying felsic host into mafic magma during magma mixing and mingling (Jayananda et al. 2014). Bladed biotite (Fig. 6a) is evidence for rapid growth and physical restriction under a super-cooling environment and is also associated with magma mixing (Hibbard 1981; Jeen et al. 2002). Random crystallization of acicular-shaped apatite crystals noticed in quartz and alkali feldspar (Fig. 6f) indicates rapid crystallization during the magma mingling (Hibbard 1991; Kumar 1995). Thus, the observed microstructures from the SGP constrained the magma mixing, mingling and undercooling.

CSD Evidence for Magma Mixing and Mingling

CSD theory is one of the most vital approaches to infer magma chamber procedure, residence period, and the mixing process (Cashman and Marsh 1988; Marsh 1998). In SGP, the core granite sample exhibits a slightly curved nature due to the successive period of cooling during magma emplacement (Fig. 8a). The temperature of the hot mafic magma quickly declines due to injection into the significantly cool crystallizing felsic host during interaction. When the temperature decreases, it gives a sequence of straight lines with the same slope but different intercepts (Higgins 2006). A straight and nearly straight CSD curves (Fig.8 c and e) of MME and syn-plutonic dyke crystals likely imply thermal equilibrium during the interaction of mafic and felsic magma. The margins of granite, MMEs, and syn-plutonic dyke sample plagioclase crystals produced curved or nearly curved CSD lines (Fig.8b, d, and f) with significant fit indicate magma mixing/mingling. However, in the CSD plot of this pluton, the marginal fine-grained mafic rock crystals exhibit steeply sloping lines that resemble low growth rate and high nucleation (Fig.8 d, and f) compared to the shallow sloping line of large-grained core samples (Fig.8 c, and e). This condition arises when relatively cooler felsic magma is

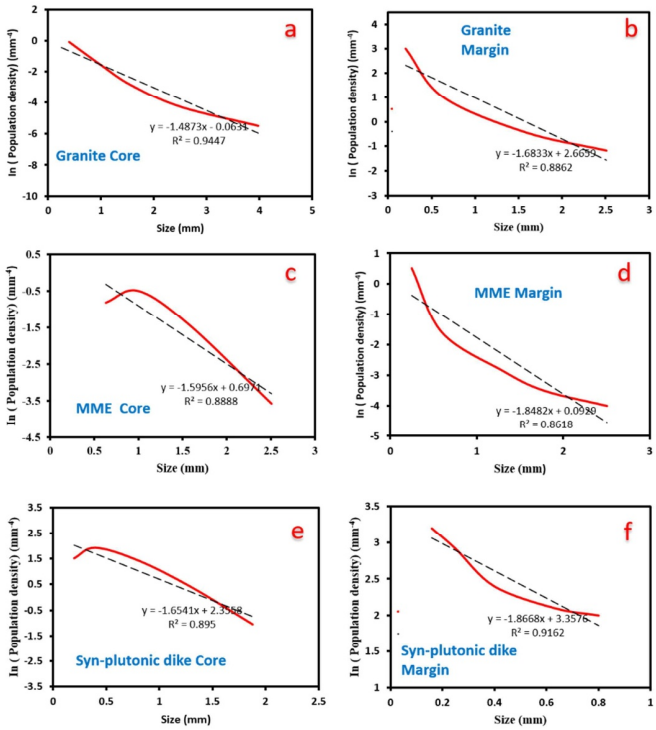

Fig. 8. Crystal size distribution study of plagioclase **(a–b)** host granite **(c-d)** MME; **(e-f)** syn-plutonic dike.

intruded by hotter mafic magma, which leads to undercooling. The calculated average residence time from CSD slopes of 100 plagioclase crystals is 170-213 years (Table 1). Further, the calculated residence time of margin samples are slightly less (J-19, AMP, and SG-13) compared to core samples (MU-15, MU-25, and J-11) due to rapid crystallization.

CONCLUSIONS

- Mafic microgranular enclaves within the Sirsilla Granite Pluton (SGP) exhibit rounded to ellipsoidal shapes along sharp to diffusive contacts with host granitoid, indicating the coeval nature of felsic and mafic magmas.
- The presence of acicular apatite and unusual bladed biotites represents to rapid crystallization in the under cooling environment associated with the magma mixing process.
- Additionally, the ocellar quartz, poikilitic feldspar, and resorbed plagioclase from the MMEs indicate disequilibrium crystallization of these crystals, which may be caused due to the magma mixing process.
- Curves of CSD plots for plagioclase crystals present in SGP rocks reveal the interaction of felsic and mafic magmas as well as sequential periods of cooling.
- The residence time of SGP samples displays distinct variation from margin to the core. The marginal samples show low residence time compared to the core samples.

Acknowledgements: The authors are thankful to Director; CSIR-NGRI for permitting to publish this work. This work forms part of the Ph.D. thesis of the first author. I acknowledge the UGC-RGNF Fellowship and MoES project to carry out this work. We particularly acknowledge the contributions of Dr. EVSSK Babu for numerous helpful discussions. The authors are grateful to the anonymous reviewer for the constructive suggestions, comments and for efficient handling.

References

Armienti, P., Pareschi, MT., Innocenti, F., Pompilio, M. (1994) Effects of magma storage and ascent on the kinetics of crystal growth - The case of the 1991-93 Mt. Etna eruption. Contrib. Mineral. Petrol., v.115, pp.402–414. doi:10.1007/BF00320974

Arvin, M., Dargahi, S., Babaei, AA. (2004) Mafic microgranular enclave swarms in the Chenar granitoid stock, NW of Kerman, Iran: Evidence for magma mingling. Jour. Asian Earth Sci., v.24, pp.105–113.

Barbarin, B. (2005) Mafic magmatic enclaves and mafic rocks associated with some granitoids of the central Sierra Nevada batholith, California: Nature, origin, and relations with the hosts. Lithos., v.80, pp.155–177. doi:10.1016/j.lithos.2004.05.010

Barbarin, B. (1990) Granitoids: Main petrogenetic classifications in relation to origin and tectonic setting. Geol. Jour., v.25, pp.227–238. doi:10.1002/gj.3350250306

Barbarin, B. and Didier, J. (1992) Genesis and evolution of mafic microgranular enclaves through various types of interaction between coexisting felsic and mafic magmas. Trans. Royal Soc. Edinb. Earth Sci., v.83, pp.145–153. doi:10.1017/S0263593300007835

Baxter, S. (2002) Field and petrographic evidence for magma mixing and mingling in Granitoids: Examples from the Galway Granite, Connemara. Mineral. Petrol., v.76, pp.63–74. doi:10.1007/s00710-001-0178-8

Cashman, K.V. (1993) Relationship between plagioclase crystallization and cooling rate in basaltic melts. Contrib. Mineral. Petrol., v.113, pp.126–142. doi:10.1007/BF00320836

Cashman, K V., Marsh, BD. (1988) Crystal size distribution (CSD) in rocks and the kinetics and dynamics of crystallization II: Makaopuhi lava lake. Contrib. Mineral. Petrol., v.99, pp.292–305. doi:10.1007/BF00375363

Castro, A., Moreno Ventas. I., de la Rosa., J.D. (1990) Microgranular enclaves as indicators of hybridization processes in granitoid rocks, Hercynian Belt, Spain. Geol Jour.,v. 25, pp.391–404. https://doi.org/10.1002/gj.3350250321

Deb, T., Bhattacharyya, T. (2018) Interaction between felsic granitoids and mafic dykes in Bundelkhand Craton: A field, petrographic and crystal size distribution study. Jour. Earth Syst. Sci., v. 127:. https://doi.org/10.1007/s12040-018-1003-7

Dey, S. (2013) Evolution of Archaean crust in the Dharwar craton: The Nd isotope record. Precambrian Res., v.227, pp.227–246. https://doi.org/10.1016/j.precamres.2012.05.005

Slaby and G. (2004) Feldspar crystallization under magma-mixing conditions shown by cathodoluminescence and geochemical modelling – a case study from the Karkonosze pluton (SW Poland). Mineral Mag., v.68, pp.561–577. https://doi.org/10.1180/0026461046840205

Elangovan, R., Krishna, K., Vishwakarma, N. (2017) Interaction of coeval felsic and mafic magmas from the Kanker Granite, Pithora region, Bastar Craton, central India. Jour Earth Syst Sci., v.126, pp.1–15. https://doi.org/10.1007/s12040-017-0886-z

Frost, TP., Mahood, GA., (1987) Field, chemical, and physical constraints on mafic- felsic magma interaction in the Lamarck Granodiorite, Sierra Nevada, California (USA). Geol Soc Am Bull., v.99, pp.272–291. https://doi.org/10.1130/0016-7606(1987)99<272:FCAPCO>2.0.CO;2

Garrido, CJ., Kelemen, PB., Hirth, G. (2001) Variation of cooling rate with depth in lower crust formed at an oceanic spreading ridge: Plagioclase crystal size distributions in gabbros from the Oman ophiolite. Geochemistry, Geophys Geosystems., v.2. https://doi.org/10.1029/2000GC000136

Hibbard, MJ. (1981) The magma mixing origin of mantled feldspars. Contrib to Mineral Petrol., v.76, pp.158–170. https://doi.org/10.1007/BF00371956

Hibbard, MJ. (1991) Textural anatomy of twelve magma-mixed granitoid systems. Enclaves Granite Petrol Dev Pet., v.32, pp.431–444.

Higgins, MD. (1996) Magma dynamics beneath Kameni volcano, Thera, Greece, as revealed by crystal size and shape measurements. Jour. Volcanol Geotherm Res., v.70, pp.37–48. https://doi.org/10.1016/0377-0273(95)00045-3

Higgins, MD. (2006) Quantitative Textural Measurements in Igneous and Metamorphic Petrology.

Higgins, MD. (2002) Closure in crystal size distributions (CSD), verification of CSD calculations, and the significance of CSD fans. Am Mineral., v.87, pp.1242–1243

Higgins, MD., Roberge, J. (2007) Three magmatic components in the 1973 eruption of Eldfell volcano, Iceland: Evidence from plagioclase crystal size distribution (CSD) and geochemistry. Jour Volcanol Geotherm Res., v.161, pp.247–260. https://doi.org/10.1016/j.jvolgeores.2006.12.002

Jayananda, M., Aadhiseshan. KR., Kusiak, MA. (2020) Multi-stage crustal growth and Neoarchean geodynamics in the Eastern Dharwar Craton, southern India. Gondwana Res., v.78, pp.228–260. https://doi.org/10.1016/j.gr.2019.09.005

Jayananda, M., Gireesh, R V., Sekhamo, KU., Miyazaki, T. (2014) Coeval felsic and Mafic Magmas in neoarchean calc-alkaline magmatic arcs, Dharwar craton, Southern India: Field and petrographic evidence from mafic to Hybrid magmatic enclaves and synplutonic Mafic dykes. Jour. Geol. Soc. India., v.84, pp.5–28. https://doi.org/10.1007/s12594-014-0106-2

Jayananda, M., Miyazaki, T., Gireesh, RV. (2009) Synplutonic mafic dykes from late archaean granitoids in the Eastern Dharwar Craton, southern India. Jour. Geol. Soc. India., v.73, pp. 117–130. doi:10.1007/s12594-009-0007-y

Jayananda, M., Tsutsumi, Y., Miyazaki, T. (2013) Geochronological constraints on Meso- and Neoarchean regional metamorphism and magmatism in the Dharwar craton, southern India. Jour Asian Earth Sci., v.78, pp.18–38. doi:10.1016/j.jseaes.2013.04.033

Jeen, M.J., Kim. J.S., Lee, J.D. (2002) Study on the origin of rapakivi texture in Bangeojin granite. Jour. Petrol. Soc. Korea., v.11, pp.30–48.

Kumar, S. (1995) Microstructural evidence of magma quenching inferred from microgranular enclave hosted in Hodruša granodiorite, western Carpathians. Geol. Carpathica., v.46, pp.379–382.

Kumar, S. (2020) Schedule of Mafic to Hybrid Magma Injections Into Crystallizing Felsic Magma Chambers and Resultant Geometry of Enclaves in Granites: New Field and Petrographic Observations From Ladakh Batholith, Trans-Himalaya, India. Front. Earth Sci., v.8. doi:10.3389/feart.2020.551097

Kumar, S. (2010) Mafic to hybrid microgranular enclaves in the Ladakh batholith, northwest Himalaya: Implications on calc-alkaline magma chamber processes. Jour. Geol. Soc. India, v.76, pp.5–25. doi:10.1007/s12594-010-0080-2

Kumar, S., Pieru, T., Rino, V. and Hayasaka, Y. (2017) Geochemistry and U–Pb SHRIMP zircon geochronology of microgranular enclaves and host granitoids from the South Khasi Hills of the Meghalaya Plateau, NE India: evidence of synchronous mafic–felsic magma mixing–fractionation and diffusion in a post-collision tectonic environment during the Pan-African orogenic cycle. Geol. Soc., London, Spec. Publ., v.457(1), pp.253-289.

Kumar, S., Rino, V., Pal, A.B. (2004) Typology and geochemistry of microgranular enclaves hosted in Malanjkhand granitoids, Central India. Jour. Geol. Soc. India, v.64, pp.277–292.

Manikyamba, C. and Kerrich, R. (2012) Eastern Dharwar Craton, India: Continental lithosphere growth by accretion of diverse plume and arc terranes. Geosci Front., v.3, pp.225–240. doi:10.1016/j.gsf.2011.11.009

Manikyamba, C., Kerrich, R., Khanna, T.C. (2009) Enriched and depleted arc basalts, with Mg-andesites and adakites: A potential paired arc-back-arc of the 2.6 Ga Hutti greenstone terrane, India. Geochim. Cosmochim. Acta, v.73, pp.1711–1736. doi:10.1016/j.gca.2008.12.020

Marsh, B.D. (1998) On the interpretation of crystal size distributions in magmatic systems. Jour. Petrol., v.39, pp.553–599. doi:10.1093/petroj/39.4.553

Meen, J.K., Rogers, J.J.W., Fullagar, P.D. (1992) Lead isotopic compositions of the Western Dharwar craton, southern India: Evidence for distinct Middle Archean terranes in a Late Archean craton. Geochim. Cosmochim. Acta, v.56, pp.2455–2470. doi:10.1016/0016-7037(92)90202-T

Meshram, T., Dora, M.L., Baswani, S.R. (2021) Petrogenesis and U-Pb geochronology of charnockites flanking the Pranhita Godavari rift in peninsular India-link between the Bastar and Eastern Dharwar Cratons. Gondwana Res., v.92, pp.113–132. doi:10.1016/j.gr.2020.12.024

Perugini, D. and Poli, G. (2012) The mixing of magmas in plutonic and volcanic environments: Analogies and differences. Lithos., v.153, pp.261–277.

Perugini, D., Poli, G., Christofides, G. and Eleftheriadis, G. (2003) Magma mixing in the Sithonia Plutonic Complex, Greece: Evidence from mafic microgranular enclaves. Mineral. Petrol., v.78, pp173–200. doi:10.1007/s00710-002-0225-0

Perugini, D., Ventura, G., Petrelli, M., Poli, G. (2004) Kinematic significance of morphological structures generated by mixing of magmas: A case study from Salina Island (southern Italy). Earth Planet Sci Lett., v.222, pp.1051–1066. https://doi.org/10.1016/j.epsl.2004.03.038

Poli, G., Tommasini, S., Halliday, AN. (1996) Trace element and isotopic exchange during acid-basic magma interaction processes. Trans R Soc Edinburgh, Earth Sci., v.87, pp.225–232. https://doi.org/10.1017/s0263593300006635

Prabhakar, BC., Jayananda, M., Shareef M, Kano T. (2009) Synplutonic mafic injections into crystallizing granite pluton from gurgunta area, northern part of eastern dharwar craton: Implications for magma chamber processes. Jour. Geol. Soc. India., v.74, pp.171–188. doi:10.1007/s12594-009-0120-y

Rajesham, T., Rao, Y.J.B. and Murti, K.S. (1993) The Karimnagar granulite terrane - a new sapphirine bearing granulite province, south India. Jour Geol Soc India., v.41, pp.51–59.

Shukla, S., Mohan, M.R. (2019) Magma mixing in Neoarchean granite from Nalgonda region, Eastern Dharwar Craton, India: Morphological, mineralogical and geochemical evidences. Jour. Earth Syst. Sci., v.128, pp.1–27. doi:10.1007/s12040-019-1095-8

Sparks, R.S.J. and Marshall, L.A. (1986) Thermal and mechanical constraints on mixing between mafic and silicic magmas. Jour. Volcanol. Geotherm. Res., v.29, pp.99–124. doi:10.1016/0377-0273(86)90041-7

Vernon, R.H. (2016) Rapakivi granite problems: plagioclase mantles and ovoid megacrysts. Aust Jour Earth Sci., v.63, pp.675–700. doi:10.1080/08120099.2016.1241953

Vernon, R.H. (1991) Interpretation of microstructures of microgranitoid enclaves. *In:* Enclaves and Granite Petrology, Dev. Petrol. Elsevier, Amsterdam 13. pp. 277–291.

Wiebe, R.A., Hawkins, D.P. (2015) Growth and impact of a mafic-silicic layered intrusion in the Vinalhaven intrusive complex, Maine. Jour. Petrol., v.56, pp.273–298. doi:10.1093/petrology/egu078

Wyllie, P.J. (1977) Crustal anatexis: An experimental review. Tectonophysics, v.43, pp.41–71. doi:10.1016/0040-1951(77)90005-1